AUT Journal of Electrical Engineering

AUT J. Elec. Eng., 51(2) (2019) 139-152
DOI: 10.22060/eej.2019.16001.5273

# The Optimal Power Flow of Multiple Energy Carriers in Networked Multi-Carrier Microgrid

V. Amir[1], M. Azimian[2, *]

[1]Assistant Professor, Department of Electrical and Computer Engineering, Kashan Branch, Islamic Azad University, Kashan, Iran.
[2]Ph.D. Student, Department of Electrical and Computer Engineering, Kashan Branch, Islamic Azad University, Kashan, Iran.

**ABSTRACT:** The future distribution network comprising different energy carriers will include small-scale energy resources (SSERs) and loads, known as a Networked multi-carrier microgrid (NMCMG). This concept not only leads to an efficient reduction in operation costs, but also encompasses the energy transformation between gas and electric networks at combined nodes, as well as district heating networks. In this paper, the combined natural gas and electricity optimal power flow (GEOPF) is employed to represent the inter-area transmission networks. The optimal GEOPF of NMCMG, which is represented as an energy hub system, is formulated as an optimization problem that is solved by applying a mixed-integer nonlinear programming (MINLP) technique. The proposed model is capable of minimizing the system costs by utilizing various sources and integrating the multiple-energy infrastructures as well as handling the energy management of the network. Simulations are performed on a system with three microgrids including combined heat and power (CHP), photovoltaic arrays, wind turbines, and energy storages in order to fulfill the required multiple demands. In the proposed model, microgrids are in grid-connected mode in order to exchange power when required. The results of the simulation demonstrate that GEOPF guarantees the regulation of power demand and power transaction in the multi-carrier microgrid (MCMG) and the main grid.

**Review History:**
Received: 2019-03-14
Revised: 2019-08-10
Accepted: 2019-08-14
Available Online: 2019-12-01

**Keywords:**
Cooperative operation
energy hub system
multi-carrier microgrid
optimal power flow
small-scale energy resources

## 1. Introduction

Considering the development in technology and the growth of energy consumption, along with the penetration of renewable energies in the distribution network, many surveys have investigated the optimal utilization of the existing network equipment along with loss reduction and improvement in reliability [1,2].

Future energy networks that support the communication infrastructure between equipment and distributed energy resources (DERs) are called smart grids [3]. However, a small district of energy network along with SSERs including renewable or non-renewable energy sources like photovoltaic (PV), wind turbine (WT), storages, and controllable/non controllable loads, is termed as microgrid (MG) [1]. MGs that include several energy carriers are known as multi-carrier microgrids (MCMGs). In the previous studies, the operation of different energy carrier infrastructures such as electricity, natural gas, and heat were studied separately, which imposed a restriction on optimal operation. However, the higher penetration of SSERs with gas consumption, particularly with co- and tri-generation, has increased the enthusiasm for using the network services among the energy carriers [4]. The concept of the energy hub system was introduced in order to define the multi-carrier system and examine the impact of one energy form on the others [5].

The expansion of the MG concept and its structure is based on the consumption in such a way that it must be able to purchase or sell energy exclusively [6]. Nowadays, the optimal operation of various energy carriers is studied autonomously. On the other hand, congestion in the transmission lines and the growth in demand have prompted scholars to find solutions for the future energy management systems. One method for effective usage of existing infrastructures inside MGs, is to consider MGs as an energy hub. To be more specific, instead of studying the various energy carriers separately, it would be better to inspect it as an integrated system [7]. This synergy ensures optimal operation and load satisfaction.

The optimal operation of the multi microgrid was studied considering uncertainties in load and DERs by Nikmehr et al. [8]. Results show that it is possible to regulate the power demand and transaction between each MG and the neighbors MG and between each MG and the main grid. Moreover, it is indicated that the power sharing between MGs with main grid can reduce the total operation cost of the future distribution network.

In [9] the optimal operation of MGs in grid-connected mode is studied while responsive loads under time-of-use (TOU) policy are considered. An economic dispatch method has been presented according to the marginal cost and optimal

*Corresponding author's email: mahdi.azimian1991@gmail.com

operation along with instantaneous energy optimization method in a stand-alone mode [10,11]. Reference [11] proposes a new control method based on the distributed approach for hybrid microgrid systems to create a network for more participation of renewable energy resources in the modern power grids. In this paper, two different objective functions are presented: total operational cost and $CO_2$ emissions. Benders decomposition is used to solve this large-scale problem. Then, a fuzzy solution is proposed to achieve the best compromise between the two objective functions. This way, both objectives can be enhanced.

Certain examples of real facilities that can be modeled as an MG include big building, university, industrial factory or a farm in a limited geographical area and it can be managed by its owner [12]. It is shown that the possibilities of cooperative operation to increase the performance efficiency in MGs can occur if the operation and the control of several homes is considered simultaneously [13–15]. By increasing the energy convertors technologies and improving the possibility of converting energy forms in the power system, the simultaneous expansion of electric and natural gas networks is studied in a few papers [16–19]. In modeling CHP systems, Arnold and Andersson [16] modeled a gas-delivery network and an electricity-generation system separately without any reliability assessment. In [20], the combined electricity and natural gas optimal power flow is considered to be a linear problem in the power system, whereas in Ref [21], the natural gas flow depends on gas pressures on both sides of the pipelines.

Reference [22] presents comparison of both mixed integer linear and continuous non-linear programing for the optimal optimization of near-zero energy buildings connected to an electric MG. The MILP method presents some scalability limits as soon as binary variables are introduced to approximate non-convex constraints rather than non-linear programing. Davatgaran et al. developed a mixed integer linear programing (MILP) model to maximize the profit of an energy hub in day-ahead energy market, including electricity selling/buying and the operational cost, using model predictive control [23]. A robust game-theoretic model is devised to handle the energy trading issue among the interconnected MGs which adopt the role of a seller or buyer depending on their specific energy necessities [24]. The proposed gaming approach is utilized to increase the possible monetary benefits or reduce the energy provision costs by giving each MG the opportunity to optimize its own benefits. Accordingly, the Nash equilibrium point is obtained for the MGs' interactions, and the uncertainty analysis in demands and wind speed are evaluated in a scenario-based technique. Unlike the heuristic methods which fail to yield a unique solution for each optimization variable, the established approach has yielded reliable and unique results in market-oriented optimization problems.

Considering the aforementioned researches, the power flow of multiple energies within a system has not been considered in the previous studies. As a consequence, the power flow of natural gas and electricity in an NMCMG is presented concurrently in this paper, with the aim of achieving an optimal generation schedule. The optimal power flow (OPC) model is adopted to represent the multi-area transmission interconnections. The fundamental electricity and natural gas modelling and their general formulations are covered to solve the DC electricity and natural gas power flow problems. It is necessary to mention that the DC OPF is used for modeling the electric network, due to its linear model and perceived advantages. In order to solve the GEOPF problem, the GEOPF problem as a mixed integer nonlinear program (MINLP) model is solved using GAMS (General Algebraic Modelling System) software. In the proposed structure, the energy generation at each MCMG, the purchased and sold energies by each MCMG, and the energy transaction among the MCMGs and the main grid are analyzed based on the operation and maintenance costs. Moreover, the network of heat among the MCMGs is considered.

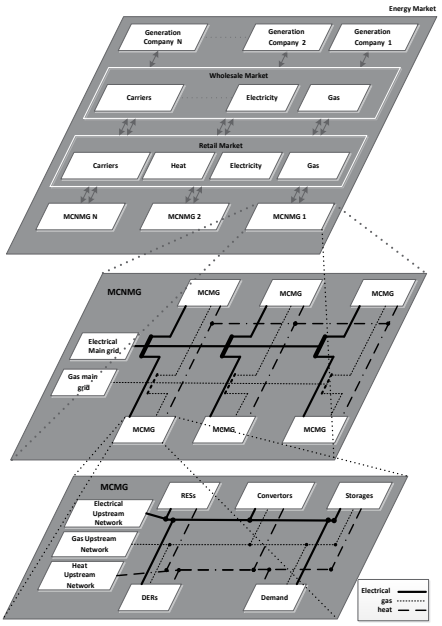


**Fig. 1. NMCMG structure**

## 2. Problem description and NMCMG architecture

The future networks consist of MGs with multiple carriers, and are termed NMCMGs. The supposed network in this work includes three MCMGs located in one geographical district, as illustrated in Fig. 1 and they have energy interactions to satisfy the various demands. An MCMG consists of an LV or MV distribution network along with networks of other energy forms such as natural gas and heat. The energy can be convert to other forms through distributed generations such as heat exchangers, co- and tri-generations, and other energy convertors. In this paper, the OPF of NMCMG is analyzed in a designed network as shown in Fig. 2. In the proposed network, the electric and natural gas networks are designed radially, whereas the district heating network is modeled as a ring network without any loss in heat transmission. To be more specific, the district heating network is represented as one single node in the NMCMG.

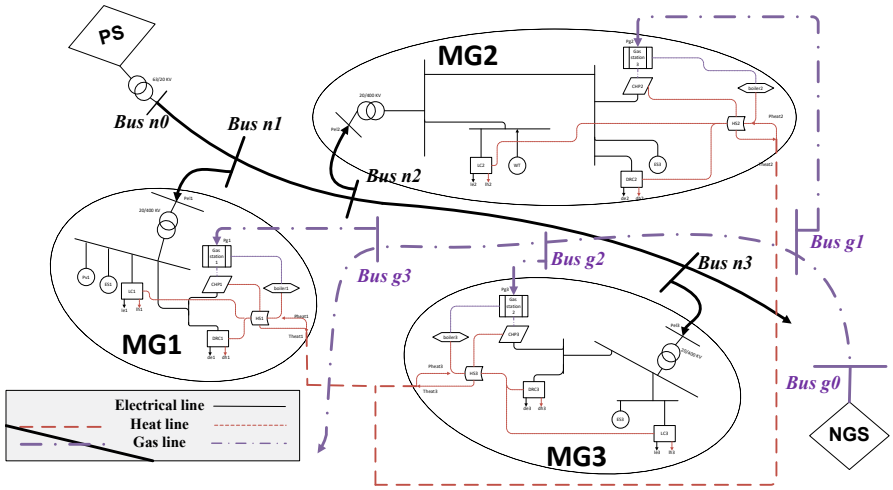


Fig. 2. Structure of the NMCMG in multi-bus model

## 3. Problem formulation

In this section, the energy scheduling in the NMCMG is carried out in a multi-bus model, with attention to the modeling of the objective function and its constraints and the DC OPF model to represent the inter area transmission network. The energy hub system to model each MCMG is used along with the various energy carriers and different equipment. The illustrated grid is connected to the main electric and gas networks via the transmission networks. The proposed model has considered the electric and heat exchanges among the MCMGs and also, the feasibility of the purchase and sale of electricity from or to the main grid.

### 3-1- Energy hub system modeling

The general structure of the energy hub system has been shown in Fig. 3. where each MCMG is modeled and represented as an energy hub system. The matrix's model of power balancing in the input and output connection points of each MCMG, based on equipment efficiencies at given intervals, is formulated as

$$L(t)+T(t)= Co\times\begin{bmatrix}P(t)\\RP(t)\end{bmatrix}- SOC(t) \tag{1}$$

Each of the proposed MCMGs is connected to the electric and natural gas main grids from two different points. The combined heat and power (CHP), boilers, and heat storage packs (SPs) exclusively used to supply heat demand are used in each MCMG. The renewable energy resources (RERs) are embedded too and enable the MCMGs to gain a high profit from selling the surplus electricity to the main grid. The electric and heat energy balance constraints in each MCMG is formulated in Eq. (2) and Eq. (3), respectively.

$$\begin{aligned}&L_e(t,m)+T_e(t,m)+M_e(t,m)=\\&P_g(t,m)\cdot\eta_e^{\,chp}(m)\cdot\upsilon^{chp}(t,m)+\\&RP_e^{Ru}(t,m)\cdot\eta_e^{\,Ru}(m)+P_e(t,m)\cdot\eta_e^{\,trans}(m)\end{aligned} \tag{2}$$

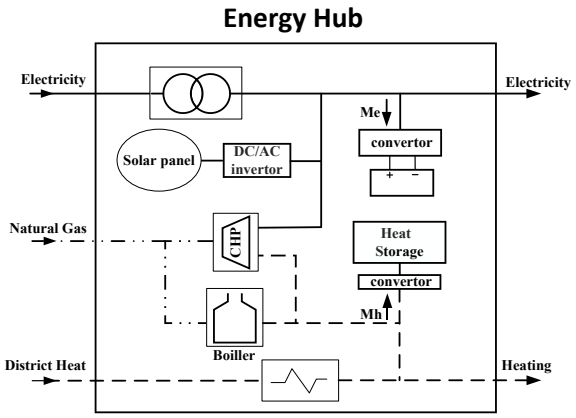


Fig. 3. Simplified Diagram of the analyzed MCMG (represented as energy hub)

$$\begin{aligned}&L_h(t,m)+T_h(t,m)+M_h(t,m)\le\\&P_g(t,m)\cdot\eta_h^{\,chp}(m)\cdot\upsilon^{chp}(t,m)+\\&P_g(t,m)\cdot\eta_h^{\,bo}(m)\cdot\upsilon^{bo}(t,m)\end{aligned} \tag{3}$$

The thermal energy generation-consumption within the NMCMG must be balanced as formulated below

$$\sum_m P_h(t,m)=\sum_m T_h(t,m) \tag{4}$$

The SPs can operate as an uninterrupted energy supply system in the MCMG. During the operation, SPs can be charged when the generation by the MCMGs is higher than the total demands and if the generation by each MCMG is lower than the total demands, the storage packs (SPs) begin to discharge. The electricity and heat energy exchange (equivalent storage flows) is stated in Eq. (5).

$$\begin{aligned}&M_l(t,m)=(E_l(t,m)-E_l(t-1,m)+E_{l,stb})\cdot\\&[I_l(t,m)\cdot\eta_l^{\,char}(m)+\frac{(1-I_l(t,m))}{\eta_l^{\,dischar}(m)}]\end{aligned} \tag{5}$$

$$E_l(1,m) = E_l(24,m) \tag{6}$$

It is assumed for the SPs that the initial charging storages are equal to the last cycle charging storages of the total capacity.

### 3-2- Electricity and natural gas network modeling

In this subsection, the GEOPF for two of the most common energy infrastructures —electricity and natural gas networks are reviewed in short. Since the electric OPF is well established, the DC OPF in an electricity network can be formulated based on the nodal power balance and the line equations. The power balance at node $n'$ in an electrical DC network for each given interval can be stated as

$$P_{bus-n}(t) - \sum_{bus-n \in N_{n'}} P_{bus-nn'}(t) = 0 \tag{7}$$

The active power flow (injection) through the transmission line $nn'$, between node $n$ and $n'$ can be obtained through Eq. (8).

$$P_{bus\_nn'}(t) = \beta_{nn'} \cdot (\delta_n(t) - \delta_{n'}(t)) \tag{8}$$

The power flow through a pipeline network can also be described by stating the nodal power balance and the line equations [20]. Similar to Eq. (8), the flow balance for an arbitrary node $n'$ for each given interval can be stated as

$$Q_{\alpha,bus-g}(t) - \sum_{bus-n \in N_{n'}} Q_{\alpha,bus-gg'}(t) = 0 \tag{9}$$

The volume flow rate injected through transmission pipeline $nn'$, between node $n$ and $n'$ for each given interval, can be calculated from Eq. (10). Flows to the connected nodes can be expressed as functions of upstream and downstream pressures. The gas pipeline model without compressor is illustrated in Fig. 4. The defined pipeline flow equation is generally valid for all types of isothermal pipeline flow (liquid and gaseous).

$$Q_{bus-gg'}(t) = Mk_{bus-gg'} \cdot Sk_{bus-gg'}(t) \cdot \sqrt{Sk_{bus-gg'}(t) \cdot (\Upsilon_{bus-g}{}^2(t) - \Upsilon_{bus-g'}{}^2(t))} \tag{10}$$

$$Sk_{bus-gg'}(t) = \begin{cases} +1 & if \quad \Upsilon_{bus-g}(t) \geq \Upsilon_{bus-g'}(t) \\ -1 & else. \end{cases} \tag{11}$$

The volume flow rate corresponding to the power flow is given by

$$Qu_{bus-gg'}(t) = GHV \cdot Q_{bus-gg'}(t) \tag{12}$$

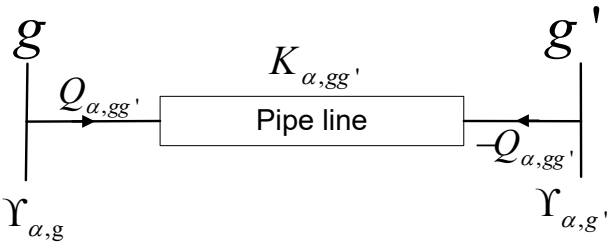


**Fig. 4. A gas pipeline model**

### 3-3- Objective function and constraints

According to the presented description of NMCMG model, the Objective function and the constraints for the centralized operation of the proposed NMCMG at the given intervals are modeled as follows

$$OF = \sum_{t=1}^{24} \left[ \sum_{p \in \{e,g\}} P_{p,tot}(t) \cdot \pi_p(t) - T_{e,tot}(t) \cdot \psi_{e,tot}(t) + \sum_{m=1}^{n_m} C_{O\&M}(t,m) \right] \tag{13}$$

The economic dispatch of the interconnected MCMGs is investigated within 24 hours. The model is a nonlinear problem in which the Objective function includes purchased and sold power in the form of various energies, in addition to the operation and maintenance (O&M) costs. The Objective function equation details are as follows

$$C_{O\&M}(t,m) = Po_e{}^{chp}(t,m) \cdot K_{O\&M}^{chp}(m) + Po_h{}^{bo}(t,m) \cdot K_{O\&M}^{bo}(m) + Po_e{}^{trans}(t,m) \cdot K_{O\&M}^{trans}(m) + \sum_{Ru} Po_e{}^{Ru}(t,m) \cdot K_{O\&M}^{Ru}(m) \tag{14}$$

$$Po_h{}^{bo}(t,m) = P_g(t,m) \cdot \eta_h{}^{bo} \cdot \upsilon^{bo}(t,m) \tag{15}$$

$$Po_e{}^{chp}(t,h) = P_g(t,m) \cdot \eta_e{}^{chp}(m) \cdot \upsilon^{chp}(t,m) \tag{16}$$

$$Po_h{}^{chp}(t,h) = P_g(t,m) \cdot \eta_h{}^{chp}(m) \cdot \upsilon^{chp}(t,m) \tag{17}$$

$$Po_e{}^{trans}(t,m) = P_e(t,m) \cdot \eta_e{}^{trans}(m) \tag{18}$$

$$Po_e{}^{Ru}(t,m) = RP_e{}^{Ru}(t,m) \cdot \eta_e{}^{Ru}(m) \tag{19}$$

$$P_{p,tot}(t) = \sum_m p_p(t,m) \tag{20}$$

$$T_{1,tot}(t) = \sum_m T_l(t,m) \tag{21}$$

To model the GEOPF correctly, the power and flow balance at each node in any electrical and natural gas network are stated in Eq. (22) to Eq. (24).

**Table. 1. Assumed values of typical NMCMG elements**

| Elements | | value | | | Unit | $K_{O\&M}$ |
|---|---|---|---|---|---|---|
| | | MG1 | MG2 | MG3 | | ($/KWh) |
| interconnector | Trans Efficiency | 0.92 | 0.90 | 0.90 | - | 0.002 |
| CHP | Capacity | 1000 | 700 | 900 | (KW) | 0.00587 |
| | Electrical Efficiency | 0.4 | 0.4 | 0.3 | - | |
| | heat Efficiency | 0.4 | 0.3 | 0.3 | - | |
| Boiler | Capacity | 1700 | 1100 | 1000 | (KW) | 0.001 |
| | heat Efficiency | 0.85 | 0.87 | 0.9 | (KW) | |
| Electricity SP | Capacity | 1-90 | 1-90 | 1-90 | (KWh) | - |
| Heat SP | Capacity | 90 | 90 | 90 | (KWh) | - |
| Inverter | Capacity | 30 | - | - | (KW) | 0.003 |
| | Efficiency | 0.95 | - | - | - | |
| WT | Efficiency | - | 0.9 | - | - | 0.1369 |

$$P_{e,tot}(t,m)-P_e(t,m)+T_e(t,m)= \sum_{n'}\beta_{bus-nn'}\left(\delta_{bus-n}(t)\_\delta_{bus-n'}(t)\right) \quad if\ \ m\to bus-n \tag{22}$$

$$P_{g,tot}(t,m)-P_g(t,m)=\sum_{g'}Sk_{bus-gg'}(t)\cdot Mk_{bus-gg'}\cdot \sqrt{Sk_{bus-gg'}(t)\cdot\left(\Upsilon_{bus-g}{}^2(t)\_\Upsilon_{bus-g'}{}^2(t)\right)} \quad if\ \ m\to bus-g \tag{23}$$

$$Sk_{bus-gg'}(t)=\begin{cases}+1 & if \quad \Upsilon_{bus-g}(t)-\Upsilon_{bus-g'}(t)\geq 0\\ -1 & else.\end{cases} \tag{24}$$

The upper and lower constraints for the allowable range and initial values of the variables are limited as follows.

$$\underline{Po_e{}^{chp}(t,m)}\leq Po_e{}^{chp}(t,m)\leq\overline{Po_e{}^{chp}(t,m)} \tag{25}$$

$$\underline{Po_h{}^{bo}(t,m)}\leq Po_h{}^{bo}(t,m)\leq\overline{Po_h{}^{bo}(t,m)} \tag{26}$$

$$\underline{P_{p,tot}(t)}\leq P_{p,tot}(t)\leq\overline{P_{p,tot}(t)} \tag{27}$$

$$\underline{T_{p,tot}(t)}\leq T_{p,tot}(t)\leq\overline{T_{p,tot}(t)} \tag{28}$$

$$\underline{E_l(l,m)}\leq E_l(l,m)\leq\overline{E_l(t,m)} \tag{29}$$

$$\underline{-M_l(t,m)}\leq M_l(t,m)\leq\overline{M_l(t,m)} \tag{30}$$

$$0\leq\upsilon^{chp}(t,m)\leq 1 \tag{31}$$

$$0\leq\upsilon^{bo}(t,m)\leq 1 \tag{32}$$

$$\upsilon^{chp}(t,m)+\upsilon^{bo}(t,m)=1 \tag{33}$$

For power systems, operation safety must be ensured so that there is no overload in the transmission branches, i.e., the power and volume flow distributions should be within the capacity limits of the transmission lines. Moreover, the voltage phase angle and up- and downstream pressures at electric and natural gas nodes must be within its lower and upper operating limits. They are mathematically formulated by

$$\left|\beta_{bus-nn'}\cdot\left(\delta_{bus-n}(t)\_\delta_{bus-n'}(t)\right)\right|\leq\overline{P_{bus-nn'}} \tag{34}$$

$$\left|S_{bus-gg'}(t)\cdot Mk_{bus-gg'}\cdot\sqrt{\left|\begin{matrix}Sk_{bus-gg'}(t)\\ \left(\Upsilon_{bus-g}{}^2(t)\_\Upsilon_{bus-g'}{}^2(t)\right)\end{matrix}\right|}\right|\leq\overline{Q_{bus-gg'}} \tag{35}$$

$$\left|\delta_{bus-n}(t)-\delta_{bus-n'}(t)\right|\leq\overline{\Delta\delta} \tag{36}$$

$$\underline{\Upsilon_{bus-gg'}}\leq\Upsilon_{bus-gg'}(t)\leq\overline{\Upsilon_{bus-gg'}} \tag{37}$$

## 4. Simulation results and discussions

In this section, the OPF and the conversion in a centralized system of interconnected MCMGs will be investigated. The optimization model is formulated as a mixed integer nonlinear program (MINLP) and is solved using GAMS software. The GEOPF is tested on the network, as shown in Fig. 3. This Figure shows the structure of an NMCMG with three MCMGs, where each one consists of SSERs, storage, and electrical and thermal loads. The three MCMGs are connected

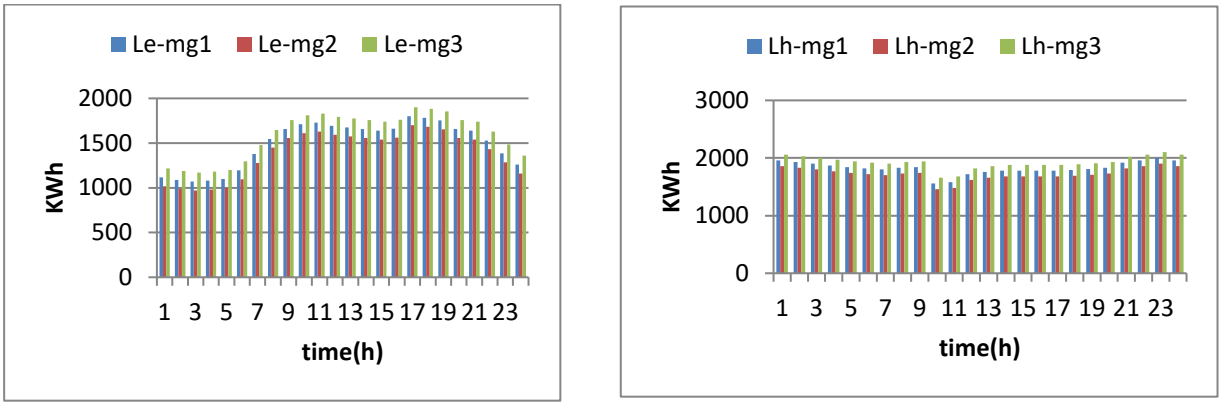


Electrical Thermal

**Fig. 5. load profile of MCMGs**

together through supposed transmission lines, where the demand of each MCMG is supplied through the main grid, but not provided by the local sources or the adjacent MCMGs. Moreover, the surplus energy can be transferred to the adjacent needy MGs or the upstream network. The MCMGs to balance the supply-demand of the district heat network are interconnected, while each MCMG is linked to the electric and natural gas main grid. So, each MCMG can buy electrical or natural gas energies from the main grid when the MCMG is unable to provide its own multiple demands from its sources. An MCMG with surplus electricity can sell its electricity to the main grid. The characteristics of the NMCMG's elements are stated in Table. 1.

The cooperative OPF of NMCMG, in the presence of SSERs, which include boiler, CHP, and RERs such as PV and WT, is the main aim of this work. The electrical and thermal load profiles in a 24-hour interval is presented in Fig. 5.

It is remarkable that the electricity purchase and sale prices are considered to be equal in three periods and the natural gas purchase prices are permanently fixed. The details are depicted in Table 2. The electricity and natural gas network data are assigned in Table 3, which includes the electrical line susceptances, transmission line and pipeline capacities, and the coefficient of the pipe and fluid properties for the main case and four scenarios. In Fig. 2, it is assumed that bus $n0$ and $g0$ serve as the reference/slack bus in the electric and natural gas network, respectively. The node $g0$ is the known-pressure node in the system which its definition is given in Ref [20]. The voltage phase angle of bus $n0$ and the gas pressure at node $g0$ are considered equal to zero and 10000 (psia), respectively.

The equivalent storage power flows and the state of charge (SOC) of electric and heat SP for MCMG1 are shown in Fig. 6.

The internal electric balance of each MCMG is depicted in Fig. 7. In Fig. 7(a, b) the power purchase is decreased in MCMG 1 and 2, owing to the generation of the RERs in some intervals and the surplus energy is sold or stored in the SPs. The demand is met by the main grid if the sources or storages

**Table. 2. Electricity and natural gas prices**

| | Time (h) | | | |
|---|---|---|---|---|
| | t1*t7 | t8*t18 | t19*t22 | t23*t24 |
| $\pi_e, \psi_e$ ($/KWh) | 0.1014 | 0.117 | 0.13 | 0.1014 |
| $\pi_g$ ($/KWh) | 0.07 | 0.07 | 0.07 | 0.07 |

are not able to satisfy the demand. As can be seen in Fig. 7(c), the electric demand in MCMG3 is supplied by the main grid in almost all intervals and the CHP and SP supply only a minor share of the energy. The total electricity balance in the network in Fig. 8 reveals a decrease in the demand for electricity purchase from the main grid for the MCMGs that have RERs. Besides, the surplus energy of MCMG 1 and 2 are sold to the main grid, except at peak intervals.

The natural gas input amount for each MCMG and the total input from the main grid to supply the natural gas-fired generation (including CHPs and boilers) are depicted in Fig. 9. This carrier has increased the flexibility of the network operation and has eventually, led to the operation being beneficial and reducing the total cost of the NMCMG.

The heat balance of the NMCMG is shown in Fig. 10. It can be observed in Fig. 10 that the most heat transfer is carried out by MCMG1 and a small share of heat energy by MCMG2. It is due to the equipment capacities and low-cost heat generation by MCMG1's equipment. The heat balance in each MCMG must be met according to the centralized operation of the MCMMG in such a way that the adjacent MCMGs must supply the heat demands of the MCMGs that need it, in case the heat is not supplied by its sources. This constraint is obviously accounted for, as shown in Fig. 11. Moreover, it is observable that the RERs have affected the boilers, causing them to be more productive than CHP in meeting the demand due to costless RER generation. Hence, the controller has more flexibility in using the boilers to fulfill the heat demand or to transfer the extra heat to the MCMGs that need it at intervals.

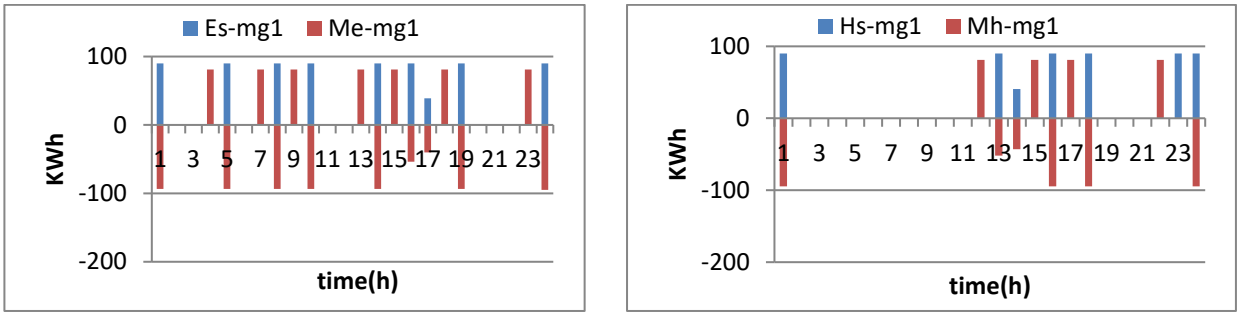


Electrical Thermal

**Fig. 6. Equivalent storage electricity flows and SOC of electric storage in MCMG1**

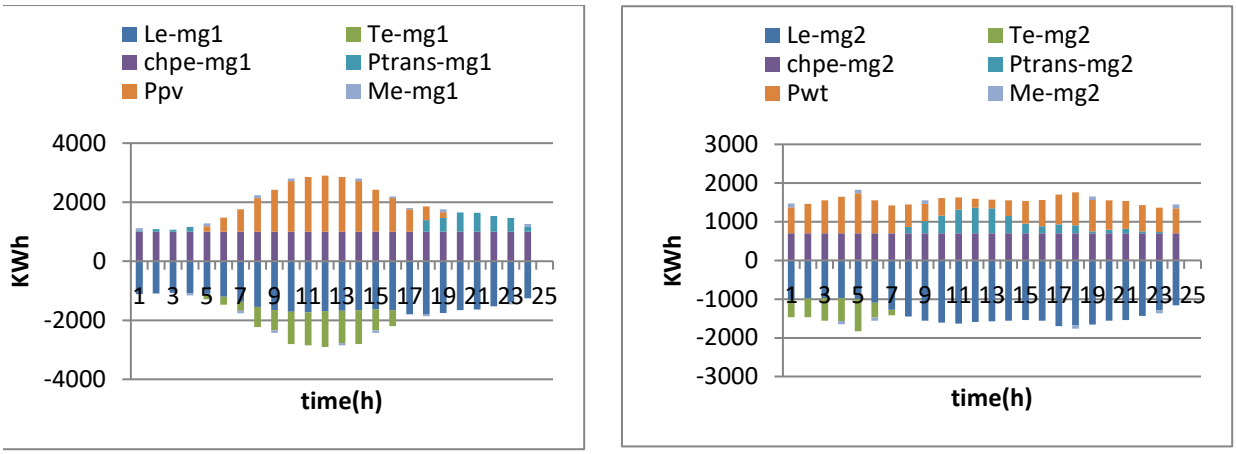


a: MCMG1 b: MCMG2

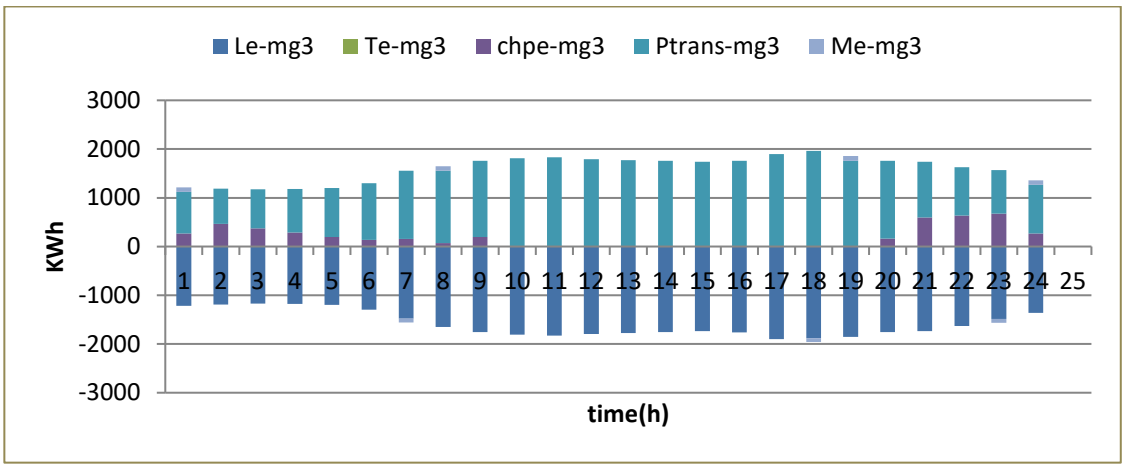


c: MCMG3

**Fig. 7. Electricity balance profiles**

The voltage phase angle and gas pressure at each electric and natural gas relevant node are illustrated in Fig. 12. According to the radial electricity and natural gas network, the voltage phase angle and gas pressure is reduced in the following buses sequentially. On the one hand, the most voltage phase angle drop has occurred at interval 18 and consequently, the network in this interval has demanded the most electric power, as shown in Fig. 8. On the other hand, the most gas pressure drop has occurred at interval 23, which was the peak for gas consumption as illustrated in Fig. 12(b). Comparing Fig. 9 and Fig. 12(b), the natural gas consumption is increased to fulfill the multiple demands by feeding the gas-fired generations and consequently, electricity purchase from the main grid is decreased.

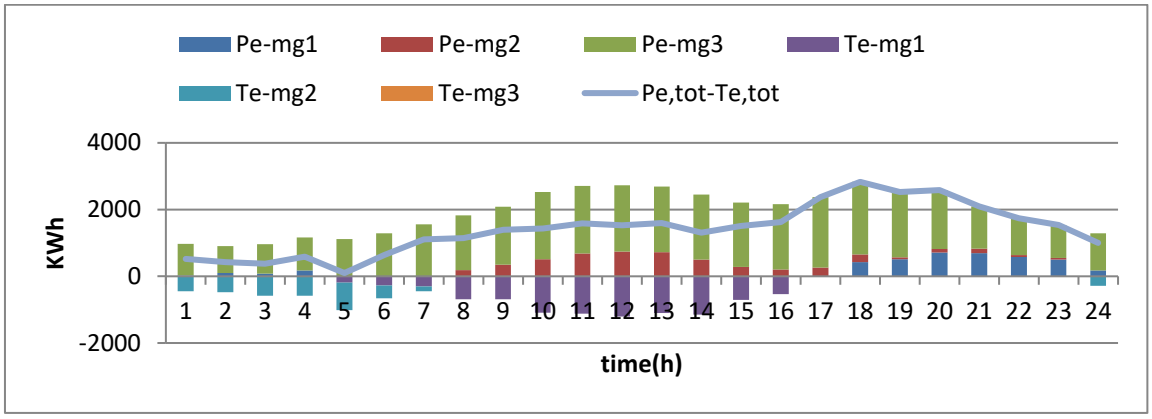


Fig. 8. Electricity balancing in NMCMG

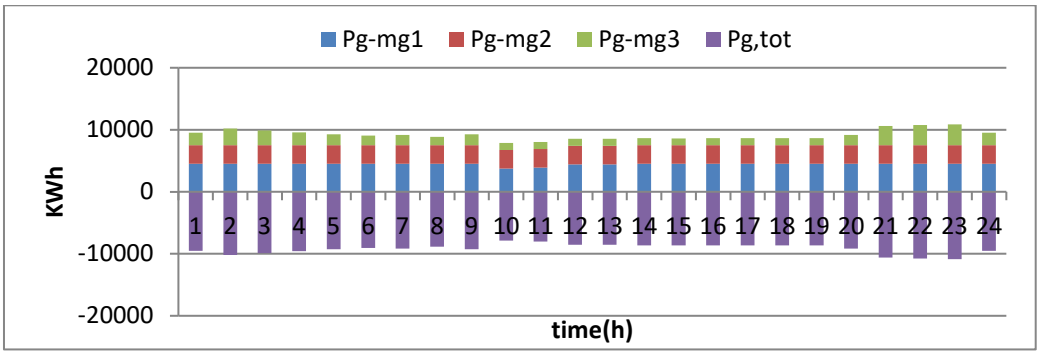


Fig. 9. Natural gas balancing in NMCMG

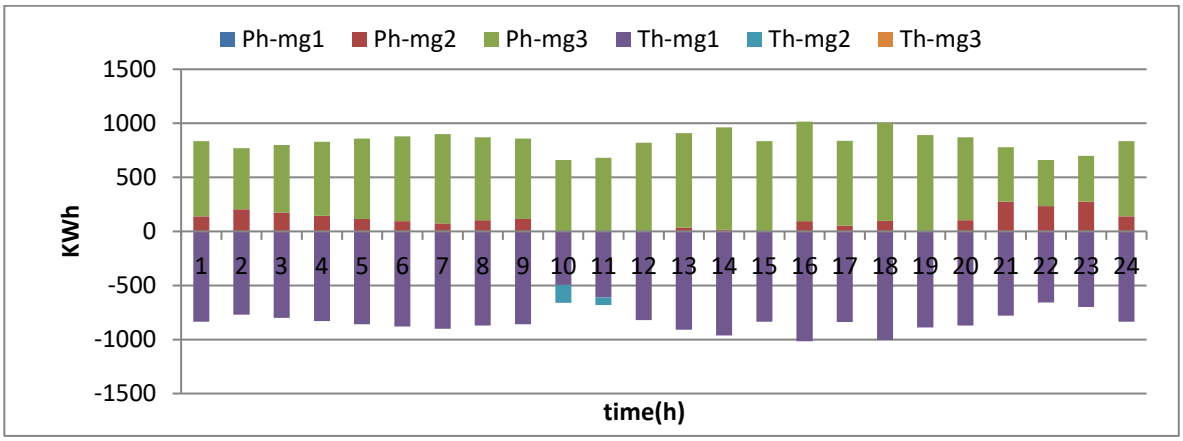


Fig. 10. Heat balance in NMCMG

The rest of this section will discuss four scenarios:

1. Limited voltage phase angle drop.
2. Limited gas pressure drop.
3. Limited capacities of the electricity transmission network.
4. Limited capacities of the natural gas transmission pipelines.

In the first scenario, considering the limited voltage phase angle drop in Table. 3, the simulation results change. Compared to the main case, in this scenario, there is less electricity purchase and more gas consumption from the main grid. This matter is proved in Fig. 13, compared with Fig. 12.

Comparing Fig. 14 and Fig. 8, it can be seen that the limited voltage phase angle drop has caused a reduction in the electricity purchase at interval 18, and as a result, the voltage phase angle worsened in most of the intervals. The limited power flow through the transmission lines has caused the gas-fired generation such as CHPs to fulfill the electrical demand. This aspect is depicted and proved in Fig. 15, particularly when compared with Fig. 9. Furthermore, owing to the gas

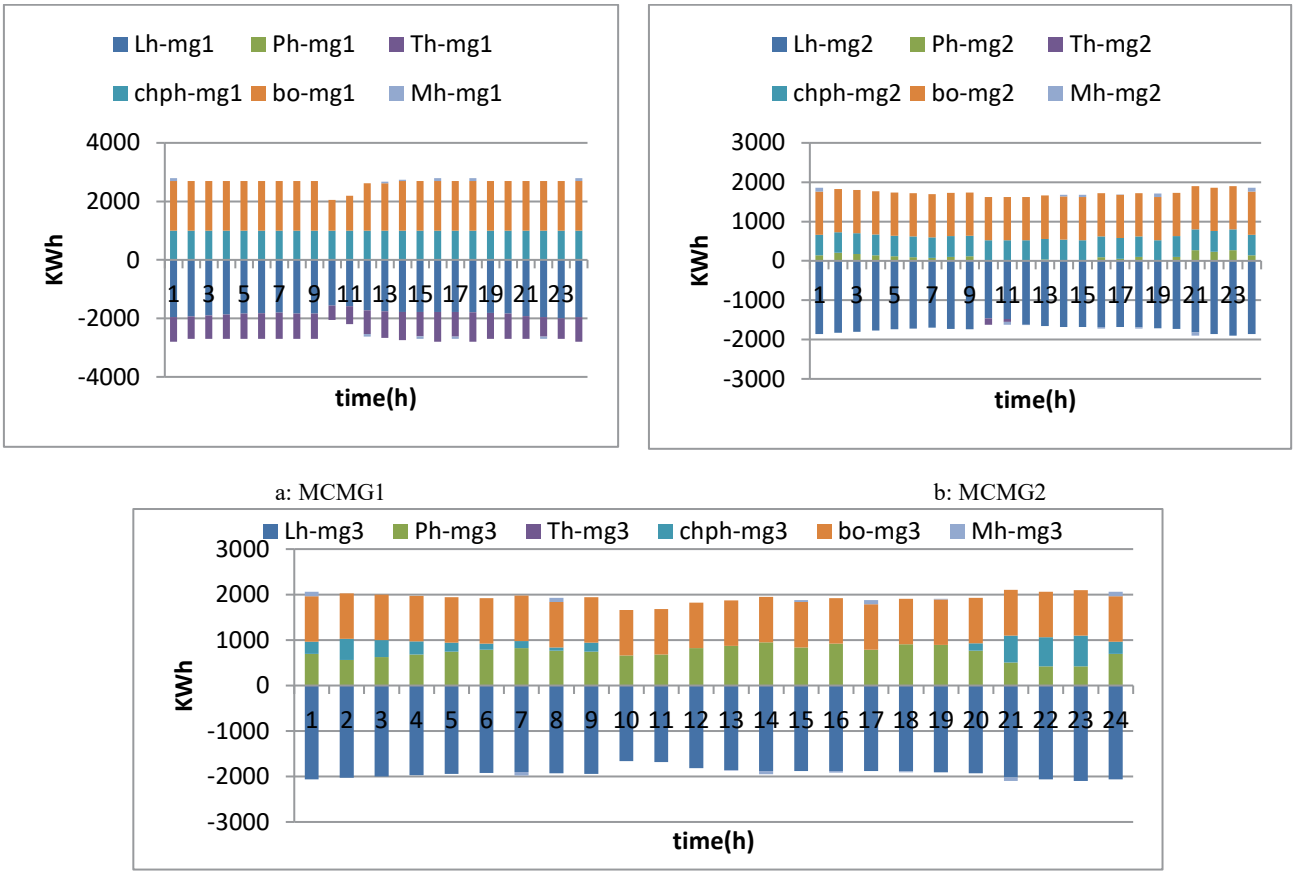


a: MCMG1 b: MCMG2

c: MCMG3

**Fig. 11. Heat balancing in MCMGs**

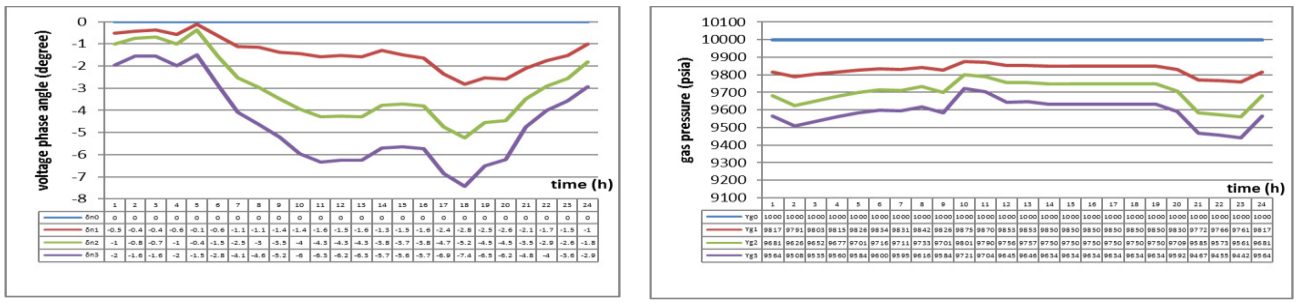


a: voltage phase angle b: gas pressure

**Fig. 12. The voltage phase angle and gas pressure at the electric and natural gas nodes.**

input increase in order to supply gas consumers like CHPs, the heat balance in NMCMG is influenced, as illustrated in Fig. 16.

In the second scenario, the gas pressure drop of the nodes is restricted, which leads to a reduction in the natural gas purchase, and supplying the electrical demand is attempted by purchasing electricity from the main grid. On the other hand, heat balance got obviously affected to satisfy the demand. In this condition, in order to overcome the problem, the performances of the SPs (particularly heat SPs) are enhanced. The equivalent storage power flows and the SOC of SPs for MCMG1 are illustrated in Fig. 17. Comparing the performance of SPs in this paper with Akhtar Hussain's in [25] declares that SPs play a crucial role in the overall performance of the NMCMG when line capacities of electrical and natural gas are appeared to be in the bottlenecks.

In Scenarios 3 and 4, the impact of the limited capacities of the electricity transmission network and the natural gas transmission pipelines, based on Table. 3, is investigated. These limitations not only affect the energy balance of the network, but also, more importantly, increases the operations cost of the NMCMG as listed in Table. 4. In Scenario 3, the

**Table. 3. The electricity and natural gas network data for the main case and its scenarios**

| | Electrical & Gas Network | | Susceptances | Mk | Main case | 1st scenario | 2nd scenario | 3rd scenario | 4th scenario |
|---|---|---|---|---|---|---|---|---|---|
| | From | To | | | Capacity limits (KWh) | Min voltage phase angle ($\delta^{\circ}$) | Min gas pressure ( $\Upsilon$ psia) | Capacity limits | |
| Electrical transmission lines | n0 | n1 | 100 | - | 10000 | -6 | - | 1800 | 10000 |
| | n1 | n2 | 100 | - | 10000 | -6 | - | 1800 | 10000 |
| | n2 | n3 | 100 | - | 10000 | -6 | - | 1800 | 10000 |
| Natural gas pipelines | g0 | g1 | - | 5 | 10000 | - | 9500 | - | 14000 |
| | g1 | g2 | - | 4 | 10000 | - | 9500 | - | 8000 |
| | g2 | g3 | - | 3 | 10000 | - | 9500 | - | 4000 |

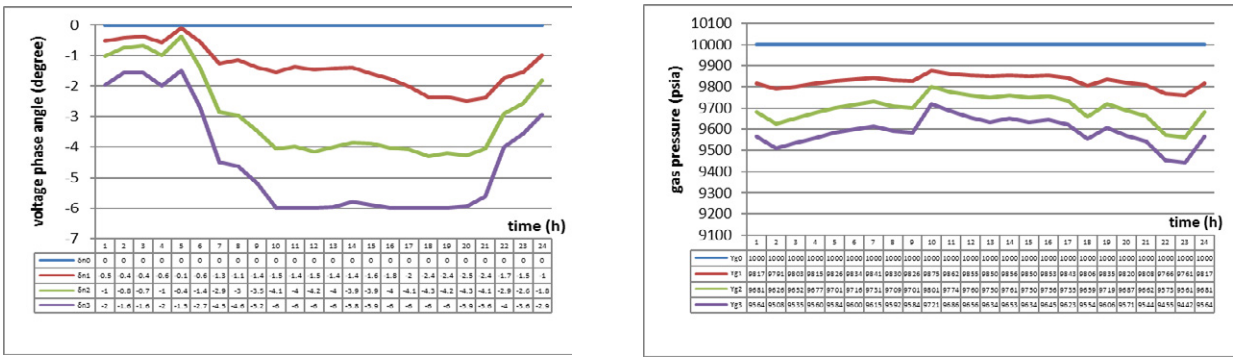


a: voltage phase angle b: gas pressure

**Fig. 13. The voltage phase angle and gas pressure at the electric and natural gas nodes for Scenario 1.**

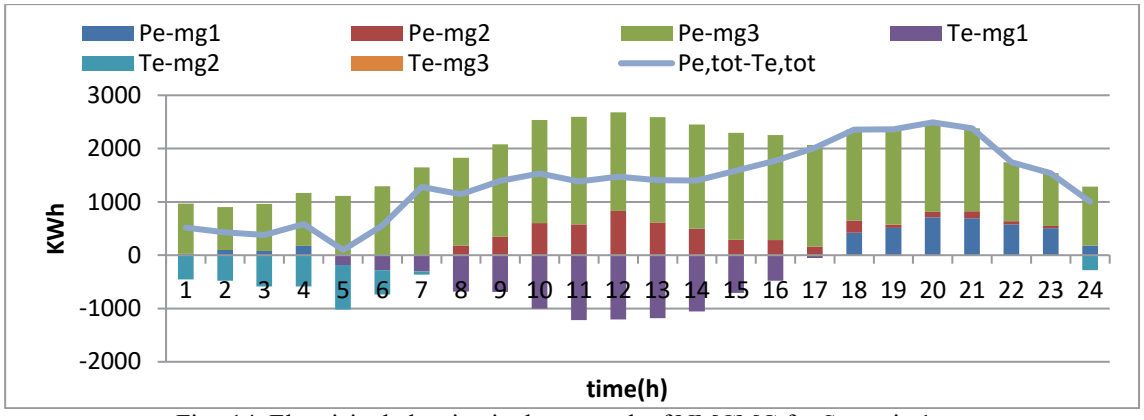


**Fig. 14. Electricity balancing in the network of NMCMG for Scenario 1**

electricity purchase from the main grid is decreased at peak intervals due to load congestion in the transmission line. Hence, the consumers of natural gas have increased their demand for energy, which has an observable impact on the heat interchange, as the results are depicted in Fig. 18 to 20.

The power flow through the transmission line for a 24-hour interval for Scenario 3 is illustrated in Table. 5. On the other hand, the gas flow through the pipelines with restricted capacity for Scenario 4 is shown in Table. 6.

Comparison of the results of this paper with Akhtar

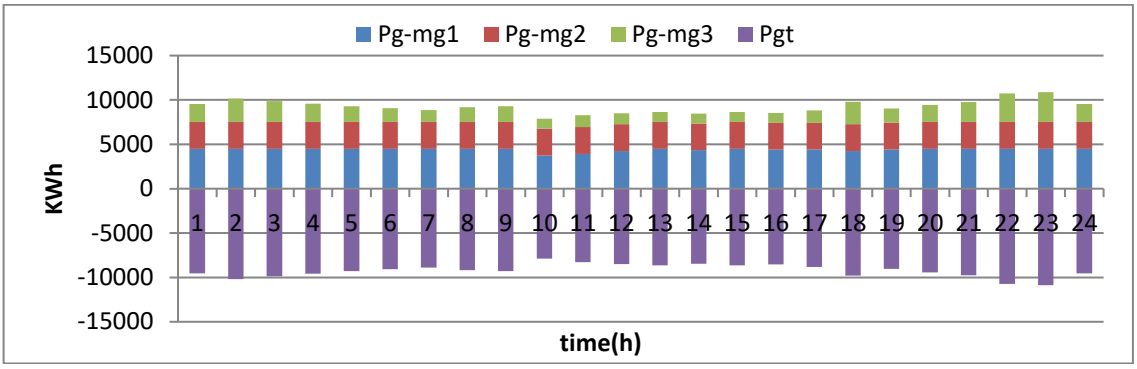


Fig. 15. Natural gas balancing in NMCMG for Scenario 1

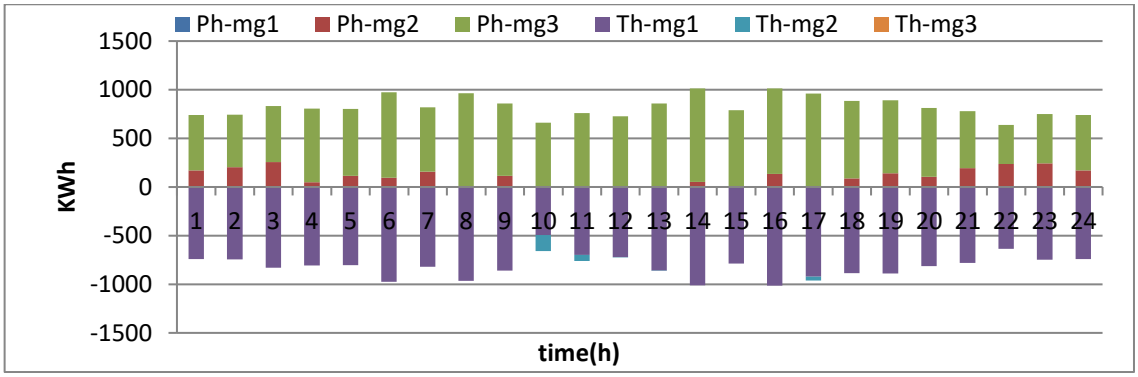


Fig. 16. Heat balance in NMCMG for Scenario 1

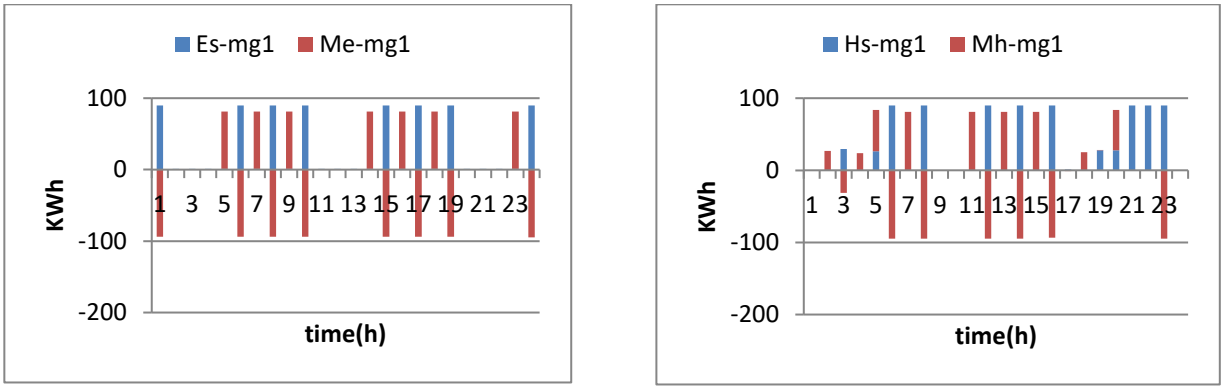


a: electrical b: thermal

Fig. 17. Equivalent storage electricity flows and SOC of storages in MCMG1 for Scenario 2.

Table. 4. Total operation costs for main case and its scenarios

| | Main case | Scenario 1 | Scenario 2 | Scenario 3 | Scenario 4 |
|---|---|---|---|---|---|
| Total cost ($) | 19929.48 | 19935.95583 | 19954.98615 | 20069.33421 | 20108.28689 |

Hussain's in [25] reveals that consideration of the congestion in the transmission and pipelines, particularly from the main electric and natural gas network, can complex the energy scheduling of each MCMG and results in a higher operation cost in the NMCMG. The main weakness in their study is that they made no attempt to analyze the thermal energy wastage under different scenarios of line capacities including electricity, heat, and natural gas. Scrutinizing the performance of heat balances in Fig. 16 and 20 with Fig. 8 of reference [25] manifests that the thermal energy wastage in the NMCMG can be severely escalated in case of any congestion occurrence, even in the electricity transmission

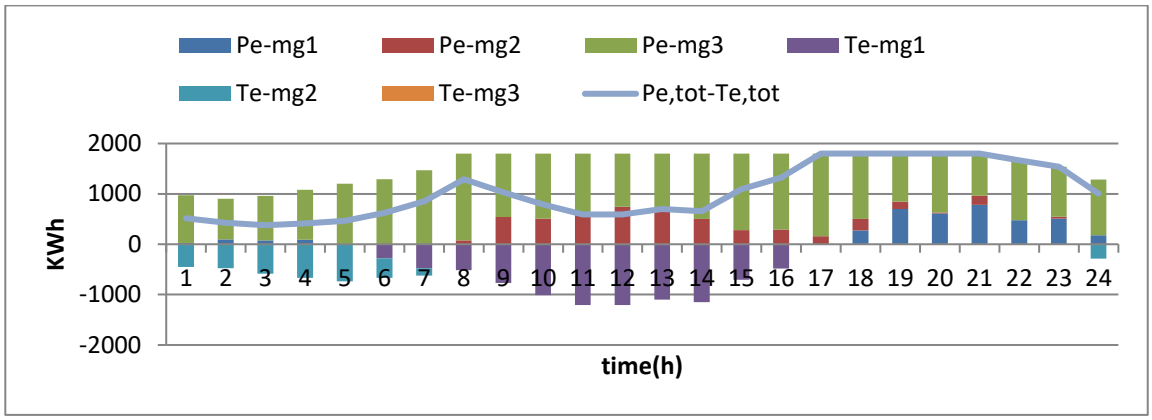


Fig. 18. Electricity balancing in NMCMG for Scenario 3

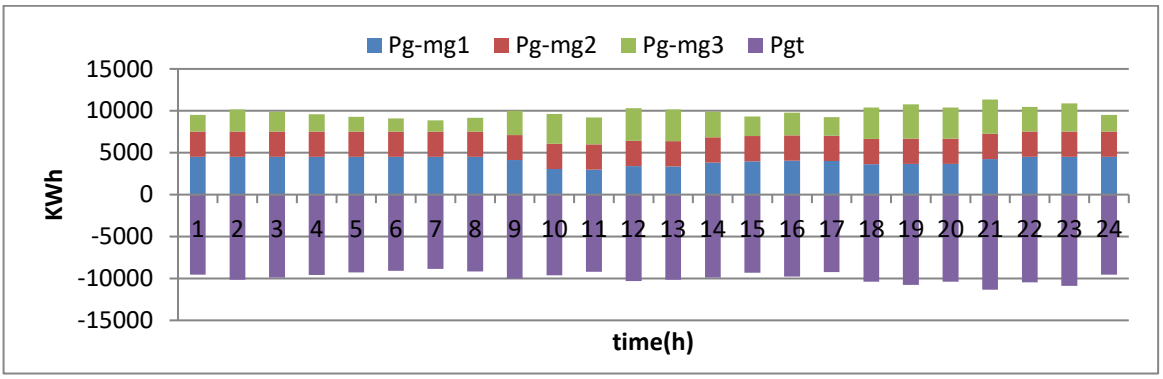


Fig. 19. Natural gas balancing in NMCMG for Scenario 3

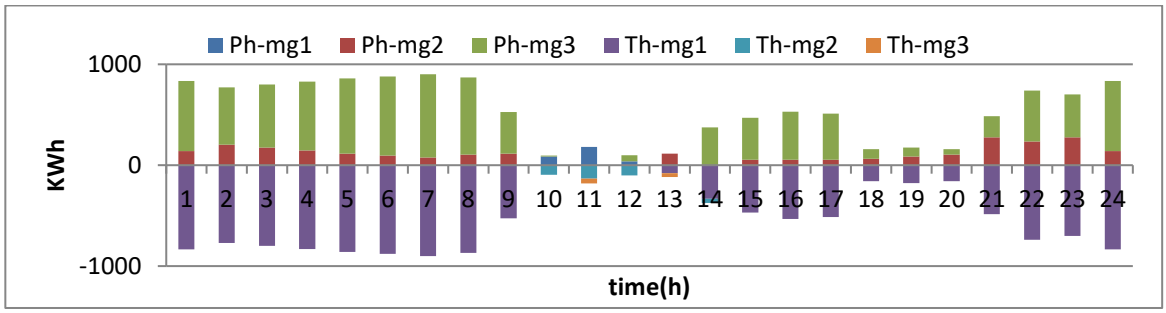


Fig. 20. Heat balance in NMCMG for Scenario 3

network. However, a considerable fall in the operation costs can be acquired considering thermal energy trading between MCMGs. Thus, the energy scheduling in each MCMG is easily managed with utilization of local DERs through connected MCMGs in demand-side resources.

## 5. Conclusion

This paper presented an approach for the combined optimization of coupled power flows of various energy infrastructures in an NMCMG environment. Moreover, the combined GEOPF model to represent the multi-area transmission interconnections was used in this work. The electric and natural gas networks were designed radially whereas the district heating network was modeled as a ring network without any loss in heat transmission. To be more specific, the district heating network was represented as one single node in the NMCMG so that the MCMGs can exchange heat. An MINLP-based model for optimal energy management of an NMCMG in a centralized network was proposed to minimize the operation and maintenance costs in the grid. The prevalent disadvantage of conventional MG structure with one form of energy was resolved by the proposed NMCMG with multiple energy carriers as compared to the prevailing electric energy management strategies. Hence, the

**Table. 5. Power flows through the transmission lines for scenario 3**

| | | Time (h) | | | | | | | | | | | | | | | | | | | | | | | |
|---|---|---|---|---|---|---|---|---|---|---|---|---|---|---|---|---|---|---|---|---|---|---|---|---|---|
| | | 1 | 2 | 3 | 4 | 5 | 6 | 7 | 8 | 9 | 10 | 11 | 12 | 13 | 14 | 15 | 16 | 17 | 18 | 19 | 20 | 21 | 22 | 23 | 24 |
| Electricity flows through lines | P,n0-n1 | 517.71 | 425.18 | 377.61 | 416.4 | 466.78 | 622.97 | 850.13 | 1288.1 | 1031 | 787.95 | 593.85 | 592 | 701.6 | 652.31 | 1093.1 | 1319.6 | 1800 | 1800 | 1800 | 1800 | 1800 | 1668.7 | 1536.8 | 1001.8 |
| | P,n1-n2 | 493.45 | 328.44 | 300.44 | 329.44 | 478.68 | 900.97 | 1326.8 | 1800 | 1800 | 1800 | 1800 | 1800 | 1800 | 1800 | 1800 | 1800 | 1800 | 1524.6 | 1098.8 | 1188.7 | 1019.4 | 1194.4 | 1030.2 | 822.23 |
| | P,n2-n3 | 946.14 | 804.44 | 884.44 | 994.44 | 1203.4 | 1291.1 | 1469.8 | 1722.9 | 1259.8 | 1288.8 | 1222.9 | 1058.8 | 1078.8 | 1298.8 | 1518.8 | 1505.8 | 1642.9 | 1294.5 | 957.01 | 1172.4 | 836.09 | 1194.4 | 990.11 | 1104.9 |

**Table. 6. Natural gas flows through the pipelines for scenario 4**

| | | Time (h) | | | | | | | | | | | | | | | | | | | | | | | |
|---|---|---|---|---|---|---|---|---|---|---|---|---|---|---|---|---|---|---|---|---|---|---|---|---|---|
| | | 1 | 2 | 3 | 4 | 5 | 6 | 7 | 8 | 9 | 10 | 11 | 12 | 13 | 14 | 15 | 16 | 17 | 18 | 19 | 20 | 21 | 22 | 23 | 24 |
| Natural gas flows through pipelines | P,g0-g1 | 9918.5 | 10146.1 | 10042.1 | 9742.1 | 9442.1 | 9242.1 | 9312.1 | 9566.3 | 8810.5 | 7964.3 | 8125.47 | 8125.4 | 8463.9 | 8343.1 | 8842.1 | 9382.1 | 9029.2 | 9376.3 | 10432. | 10046.3 | 11014.3 | 11014.3 | 11014.3 | 9722.55 |
| | P,g1-g2 | 6904.14 | 7131.82 | 7027.7 | 6727.7 | 6427.7 | 6227.77 | 6297.77 | 6551.98 | 5796.19 | 4949.93 | 5111.11 | 5111.11 | 5449.53 | 5328.65 | 5827.77 | 6367.77 | 6014.88 | 6361.98 | 7417.77 | 7031.98 | 8000 | 8000 | 8000 | 6708.18 |
| | P,g2-g3 | 4000 | 4000 | 4000 | 4000 | 4000 | 4000 | 4000 | 4000 | 4000 | 3838.8 | 4000 | 4000 | 4000 | 4000 | 4000 | 4000 | 4000 | 4000 | 4000 | 4000 | 4000 | 4000 | 4000 | 4000 |

proposed model proved to be more cost-efficient as compared to the prevailing electric energy management strategies. The result manifests that the simultaneous power flow of multiple energy infrastructures in an interconnected group of MCMGs provides an opportunity toward better operation of MCMGs when the network capacities are not adequate enough. Overall, a more economical, effective and reliable operation is derived by the proposed GEOPF model.

## Nomenclatures

| | |
|---|---|
| $C$ | cost ($) |
| $Co$ | convertor coupling matrix |
| $E$ | state of charge (storage energy) (KWh) |
| $GHV$ | gross heating value of the fluid |
| $I$ | binary variable |
| $L$ | non-controllable load (KWh) |
| $M$ | equivalent storage power flows (storage charge and discharge ramp rate) (KWh) |
| $Mk_{bus-gg'}$ | coefficient of the pipe and fluid properties |
| $P$ | input energy (KWh) |
| $P_{bus-nn'}$ | active power flow (injection) through transmission line $nn'$ (KWh) |
| $Po$ | generated energy (KWh) |
| $Q$ | the volume flow rate through pipeline $gg'$ (SCF/hr) |
| $Qu$ | natural gas power flow through a pipeline |
| $RP$ | renewable generation (KWh) |
| $T$ | transferred energy (KWh) |
| $t$ | time (hr) |

*Greek signs*

| | |
|---|---|
| $\eta$ | Efficiency |
| $\beta_{bus-nn'}$ | susceptance of the electric line joining node $n$ and $n'$ |
| $\delta_n$ | voltage phase angle (degree) |
| $\Upsilon$ | pressure at node (psia) |
| $\pi$ | energy purchase price ($/KWh) |
| $\psi$ | energy sale price ($/KWh) |
| $\upsilon$ | dispatch factor (%) |

*Superscripts*

| | |
|---|---|
| $bo$ | boiler |
| $char$ | charging power of storage interface |
| $chp$ | combined heat and power |
| $dischar$ | discharging power of storage interface |

| | |
|---|---|
| *equip* | equipment |
| *pv* | photovoltaic |
| *trans* | transformer |
| *wt* | wind turbine |

*Footnotes*

| | |
|---|---|
| 0 | base value |
| *bus* − *g* | gas node (bus) |
| *bus* − *n* | electrical node (bus) |
| *e* | electricity |
| *g* | natural gas |
| *h* | heat |
| *l* | output carrier |
| *m* | Microgrid No. |
| *O & M* | operation and maintenance |
| *p* | input carrier |
| *tot* | total |
| *stb* | standby energy losses |

## References


[1] N. Saito, T. Niimura, K. Koyanagi, R. Yokoyama, Trade-off analysis of autonomous microgrid sizing with PV, diesel, and battery storage, in: 2009 IEEE Power & Energy Society General Meeting, IEEE, 2009, pp. 1-6.

[2] A. Ipakchi, F. Albuyeh, Grid of the future, IEEE power and energy magazine, 7(2) (2009) 52-62.

[3] M. Sadiku, S. Musa, S.R. Nelatury, Smart grid—An introduction, International Journal of Electrical Engineering & Technology (IJEET), 7(1) (2016) 45-49.

[4] F. Kienzle, P. Favre-Perrod, M. Arnold, G. Andersson, Multi-energy delivery infrastructures for the future, in: 2008 First international conference on infrastructure systems and services: building networks for a brighter future (INFRA), IEEE, 2008, pp. 1-5.

[5] A. Sheikhi, A. Ranjbar, H. Oraee, Financial analysis and optimal size and operation for a multicarrier energy system, Energy and buildings, 48 (2012) 71-78.

[6] M. Shahidehpour, Our aging power systems: infrastructure and life extension issues [guest editorial], IEEE Power and Energy Magazine, 4(3) (2006) 22-76.

[7] N. Cai, N.T.T. Nga, J. Mitra, Economic dispatch in microgrids using multi-agent system, in: 2012 North American Power Symposium (NAPS), IEEE, 2012, pp. 1-5.

[8] N. Nikmehr, S.N. Ravadanegh, Optimal power dispatch of multi-microgrids at future smart distribution grids, IEEE transactions on smart grid, 6(4) (2015) 1648-1657.

[9] M. Niu, W. Huang, J. Guo, L. Su, Research on economic operation of grid-connected microgrid, Power System Technology, 34(11) (2010) 38-42.

[10] Q. Shi, G. Geng, Q. Jiang, Real-time optimal energy dispatch of standalone microgrid, Proceedings of the CSEE, 32(16) (2012) 26-35.

[11] A. Zakariazadeh, S. Jadid, P. Siano, Multi-objective scheduling of electric vehicles in smart distribution system, Energy Conversion and Management, 79 (2014) 43-53.

[12] A. Esmat, A. Magdy, W. ElKhattam, A.M. ElBakly, A novel energy management system using ant colony optimization for micro-grids, in: 2013 3rd International Conference on Electric Power and Energy Conversion Systems, IEEE, 2013, pp. 1-6.

[13] I. Koutsopoulos, L. Tassiulas, Challenges in demand load control for the smart grid, Ieee Network, 25(5) (2011) 16-21.

[14] M. Motevasel, A.R. Seifi, Expert energy management of a micro-grid considering wind energy uncertainty, Energy Conversion and Management, 83 (2014) 58-72.

[15] J.M. Guerrero, M. Chandorkar, T.-L. Lee, P.C. Loh, Advanced control architectures for intelligent microgrids—Part I: Decentralized and hierarchical control, IEEE Transactions on Industrial Electronics, 60(4) (2012) 1254-1262.

[16] M. Arnold, G. Andersson, Decomposed electricity and natural gas optimal power flow, in: 16th Power Systems Computation Conference (PSCC 08), Glasgow, Scotland, Citeseer, 2008.

[17] C.M. Correa-Posada, P. Sánchez-Martın, Security-constrained optimal power and natural-gas flow, IEEE Transactions on Power Systems, 29(4) (2014) 1780-1787.

[18] G. Koeppel, G. Andersson, The influence of combined power, gas, and thermal networks on the reliability of supply, in: Proceedings of The Sixth World Energy System Conference, 2006, pp. 10-12.

[19] A. Kargarian, B. Falahati, Y. Fu, M. Baradar, Multiobjective optimal power flow algorithm to enhance multi-microgrids performance incorporating IPFC, in: 2012 IEEE Power and Energy Society General Meeting, IEEE, 2012, pp. 1-6.

[20] S. An, Q. Li, T.W. Gedra, Natural gas and electricity optimal power flow, in: 2003 IEEE PES Transmission and Distribution Conference and Exposition (IEEE Cat. No. 03CH37495), IEEE, 2003, pp. 138-143.

[21] M. Geidl, G. Andersson, A modeling and optimization approach for multiple energy carrier power flow, in: 2005 IEEE Russia Power Tech, IEEE, 2005, pp. 1-7.

[22] V. Reinbold, V.-B. Dinh, D. Tenfen, B. Delinchant, D. Saelens, Optimal operation of building microgrids–comparison with mixed-integer linear and continuous non-linear programming approaches, COMPEL-The international journal for computation and mathematics in electrical and electronic engineering, (2018).

[23] V. Davatgaran, M. Saniei, S.S. Mortazavi, Optimal bidding strategy for an energy hub in energy market, Energy, 148 (2018) 482-493.

[24] R. Vakili, S. Afsharnia, S. Golshannavaz, Interconnected microgrids: Optimal energy scheduling based on a game-theoretic approach, International Transactions on Electrical Energy Systems, 28(10) (2018) e2603.

[25] A. Hussain, J.-H. Lee, H.-M. Kim, An optimal energy management strategy for thermally networked microgrids in grid-connected mode, International Journal of Smart Home, 10(3) (2016) 239-258.



**HOW TO CITE THIS ARTICLE**

*V. Amir, M. Azimian, The Optimal Power Flow of Multiple Energy Carriers in Networked Multi-Carrier Microgrid, AUT J. Elec. Eng., 51(2) (2019) 139-152.*

**DOI:** 10.22060/eej.2019.16001.5273